Doppler broadening of annihilation radiation of some single-element materials from the second to the sixth periods

2010 J. Phys.: Conf. Ser. 225 012027

(http://iopscience.iop.org/1742-6596/225/1/012027)

Journal of Physics: Conference Series **225** (2010) 012027 doi:10.1088/1742-6596/225/1/012027

Doppler broadening of annihilation radiation of some single-element materials from the second to the sixth periods

A Kawasuso[1], M Maekawa[1] and K Betsuyaku[2]
[1]ASRC, Japan Atomic Energy Agency, 1233, Watanuki, Takasaki, Gunma 370-1292, Japan
[2] Mizuho Information and Research Institute, 2-3, Kanda, Nishikicho, Chiyoda-ku, Tokyo 101-8843, Japan

E-mail: kawasuso.atsuo@jaea.go.jp

Abstract. The Doppler broadening of annihilation radiation spectra of some single-element materials from the second to the sixth periods measured by the coincidence technique have been compared with the theoretical calculation based on the projector-augmented wave (PAW) method. Having appropriate valence electron configurations the calculation well reproduces the measured spectra.

Introduction

Electron-positron momentum distribution obtained through the Doppler broadening of annihilation radiation (DBAR) measurement is quite useful for identifying defects species in materials since the spectrum shape reflects the elemental difference where positrons annihilate. To interpret the experimental DBAR spectra, detailed theoretical calculation is needed. It is pointed out that the ordinal pseudo-potential manner hardly calculates the realistic electron wavefunctions near core region and this is especially serious problem when calculating the DBAR spectra for transition metals [1]. To avoid this difficulty, one way is to employ the all-electron manner for calculating electronic state. In this study, we measured the DBAR spectra of some single-element materials from the second to the sixth periods and compared them with the theoretical spectra based on the projector-augmented wave (PAW) method developed by Blöhl [2] and the two-component density functional theory.

Experiment

Samples used in this study were Be polycrystals, highly oriented pyrolytic graphite (HOPG) from the second period, Mg and Al polycrystals, Si single crystals from the third period, Ti, V, Cr, Mn, Fe, Co, Ni, Cu, Zn and Ga polycrystals and Ge single crystals from the fourth period, Zr and Mo polycrystals from the fifth period, Gd, Au and Pb polycrystals from the sixth period. After electro-chemical polishing, polycrystals were annealed in appropriate temperatures to reduce defects.
A ^{22}Na positron source deposited onto a titanium film of 5 μm thick was sandwiched by two samples and coincidence Doppler broadening measurements were carried out using two high-purity Ge detectors and the FAST-ComTec MPA-Win system. In each spectrum, more than 10^7 counts were accumulated. The energy resolution was approximately 1 keV in the full width at half maximum (FWHM). Here, the Doppler energy shift of 1 keV corresponds to 3.92 mrad in angle deviation from π of two annihilation radiations and 0.54 a.u. (3.92×10^{-3} m_0c) in momentum shift.

Calculation

The DBAR spectra were calculated within the local density approximation [3]. The valence electron momentum distribution is calculated using the conventional scheme:

$$\rho_V(\mathbf{p}) = \pi r_e^2 c^2 \sum_n \left| \int e^{-i\mathbf{pr}} \Psi_+(\mathbf{r}) \Psi_n(\mathbf{r}) \sqrt{\gamma(\mathbf{r})} d\mathbf{r} \right|^2 , \quad (1)$$

where r_e is the classical electron radius, c is the speed of light, $\Psi_+(\mathbf{r})$ is the positron wave function, $\Psi_n(\mathbf{r})$ is the valence electron wavefunction of the n-th band, and $\gamma(\mathbf{r})$ is the enhancement factor. The summation was performed over all the occupied states. The core electron momentum distribution is calculated by

$$\rho_C(\mathbf{p}) = \pi r_e^2 c^2 \sum_{i,nlm} \left| \int e^{-i\mathbf{pr}} \Psi_+(\mathbf{r}) \Psi_{i,nlm}(\mathbf{r}-\mathbf{R}_i) \sqrt{\gamma(\mathbf{r})} d\mathbf{r} \right|^2 , \quad (2)$$

where $\Psi_{i,nlm}(\mathbf{r}-\mathbf{R}_i)$ represents the core electron wavefunction specified by the principal, azimuthal, and magnetic quantum numbers (nlm) for the i-th atom and $\mathbf{R}_i$ denotes the position vector. Here, we follows the Alatalo's method. That is, the positron wavefunction is assumed to be spherically symmetric and the core wavefunction is given by $\Psi_{i,nlm}(\mathbf{r})=R_{i,nl}(r)Y_{lm}(\theta,\phi)$, where $R_{nl}(r)$ is the radial part of the wavefunction and $Y_{lm}(\theta,\phi)$ is the spherical function. Consequently, Eq. (2) is rewritten as

$$\rho_C(p) = \pi r_e^2 c^2 \sum_{i,nl} (2l+1) \left| \int j_l(pr) R_{i,nl}(r) \Psi_+(|\mathbf{r}+\mathbf{R}_i|) \sqrt{\gamma(\mathbf{r})} r^2 dr \right|^2 , \quad (3)$$

after integrating on the θ and ϕ axes, where $j_l(pr)$ is the spherical Bessel function. Thus, $\rho_C(\mathbf{p})$ becomes isotropic. The total momentum distribution is given by $\rho(\mathbf{p})=\rho_V(\mathbf{p})+\rho_C(\mathbf{p})$. One-dimensional angular correlation of annihilation radiation (1D-ACAR) spectrum is obtained by integrating the total momentum density in two momentum directions. Subsequently, DBAR spectrum is obtained by convoluting the 1D-ACAR spectrum with the resolution function having a FWHM of $3.92\text{x}10^{-3}$ m_0c.
Supercells with a 1x1x1 conventional unit cell were constructed for individual crystal systems considered in this study. The valence electron wavefunctions were calculated based on the projector augmented-wave (PAW) method [2] using the ABINIT4.6.4 code [4]. The potentials and projectors were generated using the ATOMPAW code [5]. The k-point mesh was 2x2x2 or 4x4x4. The cut-off energy of the plane wave basis set was 60 Ryd. The radial part of core electron wavefunction was represented by the Slater function parameterized by Clementi and Roetti [6]. A self-consistent positron wavefunction was calculated based on the two-component density functional theory in order to minimize the energy functional. The Borónski–Nieminen enhancement factor was adopted [7].

Results and Discussion

Figure 1 shows the DBAR spectra for the Be and HOPG samples as examples of the second period elements. The electron configuration of a Be atom is given as $1s^22s^2$. We first calculated the DBAR spectrum for Be assuming 1s core electrons. However, the calculation hardly reproduced the experimental spectrum. We therefore treated 1s electrons as valence electrons. As shown by the solid curve, the experimental spectrum is well reproduced. In the case of graphite, due to the sp^2 bonding among C atoms, a layered structure is formed. Therefore, the assumption of 1s core electrons seems to be plausible. However, again the calculation with 1s core electrons failed to reproduce the experimental spectrum. The reason is that the positron wavefunction was approximated as a spherically symmetric function following the Alatalo's method despite that real positron wavefunction is anisotropically localized at the interlayer spacing [8]. Thus, by assuming 1s valence electrons, and hence considering an anisotropic positron wavefunction, the calculation reproduces the experimental spectrum. Probably, for diamond, the 1s electrons can be approximated as isotropic core electrons.
Figure 2 shows the DBAR spectrum for the Al samples as an example of the third period elements. In this case, the calculation assuming $1s^22s^22p^6$ core and $3s^23p^1$ valence electrons reproduces the experimental spectrum. A similar result was obtained for the Si samples. For the Mg samples, both 2p 3s electrons should be treated as valence electrons.

Figure 3 shows the DBAR spectra for the Ti, Fe, Cu and Ge samples as examples of the fourth period elements. From Ti to Ni, 3s and 3p electrons should be treated as valence electrons in addition to 3d and 4s electrons. From Cu to Ge, 3s and 3p electrons may be treated as core electrons. Probably, from Ti to Ni, 3d and 4s orbitals are only partially filled and hence underlying 3s and 3p wavefunctions are modulated, while, from Cu to Ge, the nature of valence electrons may be mostly determined by 3d, 4s and 4p electrons.

Figures 4 shows the experimental DBAR spectra for the V, Cr, Mn, Fe, Co, Ni, Cu, Zn, Ga and Ge samples differentiated by the spectrum for the Ti samples. It is seen that the DBAR spectra change systematically with increasing atomic number from Ti. For the V, Cr and Mn samples, the change in the spectrum shape is relatively small, but the broad bump at around $20\text{x}10^{-3}$ m_0c increases dramatically from Fe to Cu. This change corresponds to the filling of 3d bands. From Zn to Ge, the bump at around $20\text{x}10^{-3}$ m_0c decreases and the intensity at low momentum region increases. This reflects the enhancement of annihilation rate between positrons and the 4sp band electrons. Figure 5 shows the calculated differential DBAR spectra corresponding to the elements in Fig. 4. The calculation reproduces the experimental differential spectra. Although the effect of crystal structure on the DBAR spectrum shape seems to be small for bcc, fcc and hcp, the diamond structure (Ge) gives rise to a dramatic change.

Figures 6 shows the DBAR spectra for the Zr and Mo samples as examples of the fifth period elements. Similarly to the Ti and Cr in the third period, by treating 4s, 4p, 4d and 5s electrons as valence electrons, the calculation reproduces the experimental spectra. Figure 7 shows the DBAR spectra for the Gd and Pb samples as examples of the sixth period elements. In their calculations, the valence electron configurations are assumed to be $4f^{7}5s^{2}5p^{6}5d^{1}6s^{2}$ and $5d^{10}6s^{2}6p^{2}$, respectively. The calculations reproduce the experimental spectra suggesting that the assumed valence electron configurations are valid.

Conclusions

In the present work, we compared the measured and calculated DBAR spectra for a series of single element materials from the second to sixth periods. Assuming appropriate valence electron configurations, the calculation based on the PAW method for electronic state and the two-component density functional theory reproduced the measured spectra. Having this theoretical calculation, the DBAR measurement will be a useful manner for analysing electronic state of materials as well as defect identification and elemental analysis.

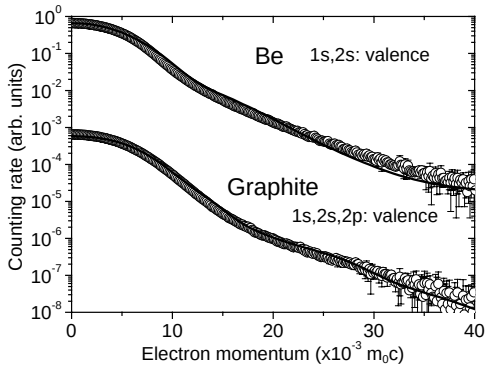

Figure 1. DBAR spectra for the Be and HOPG samples (the second period). Open circles and solid lines denote measured and calculated spectra, respectively.

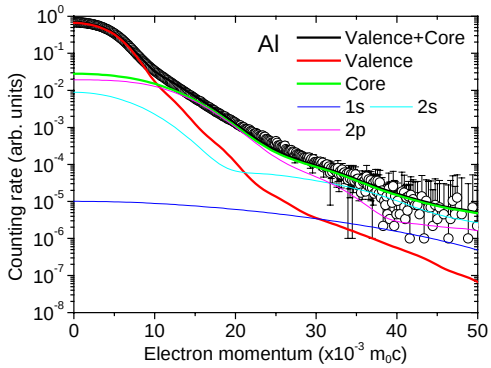

Figure 2. DBAR spectrum for the Al samples (the third period). Open circles and solid lines denote measured and calculated spectra, respectively.

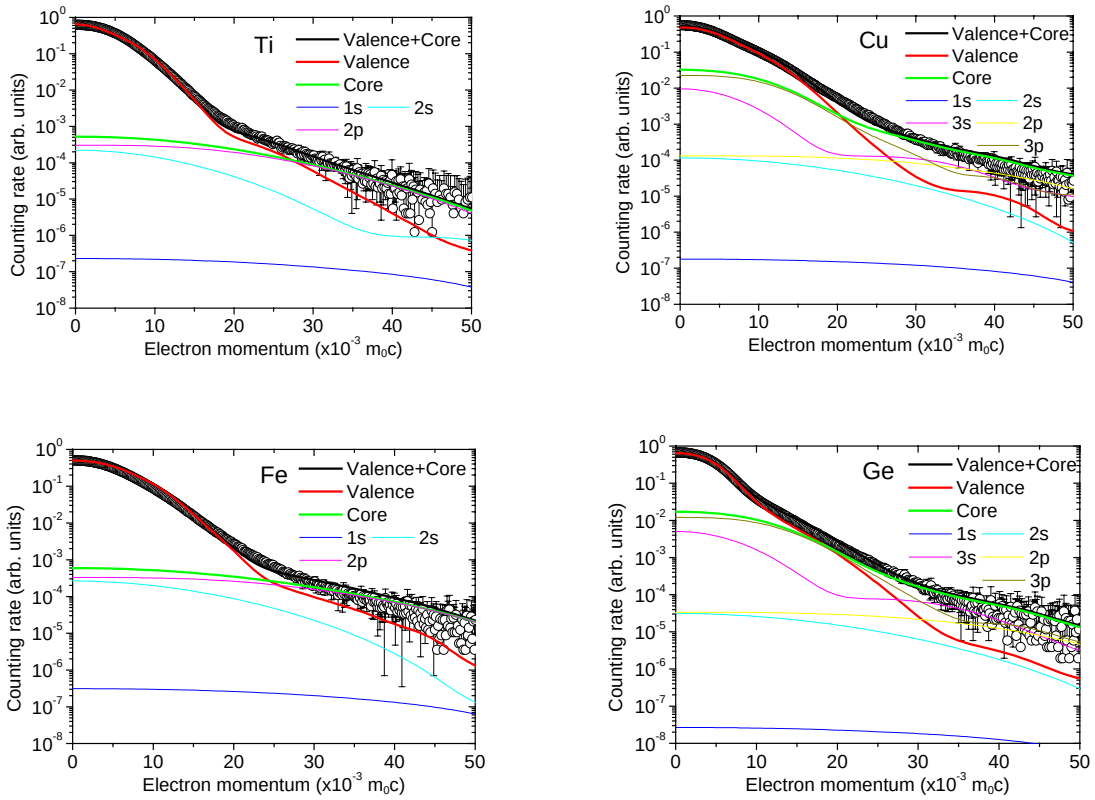

Figure 3. DBAR spectra for the Ti, Fe, Cu and Ge samples (the fourth period). Open circles and solid lines denote measured and calculated spectra, respectively.

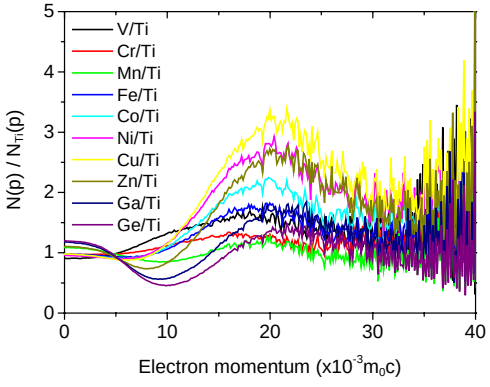

Figure 4. Experimental DBAR spectra for the V, Cr, Mn, Fe, Co, Ni, Cu, Zn, Ga and Ge samples differentiated by the spectrum for the Ti samples.

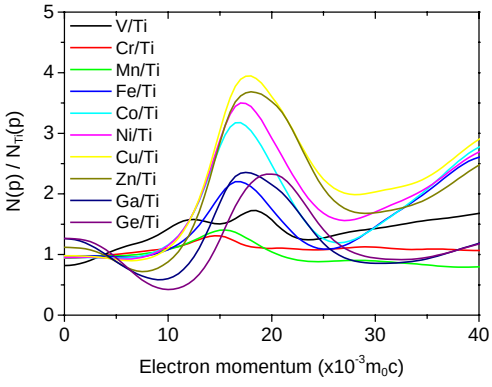

Figure 5. Calculated DBAR spectra for V, Cr, Mn, Fe, Co, Ni, Cu, Zn, Ga and differentiated by the spectrum for Ti.

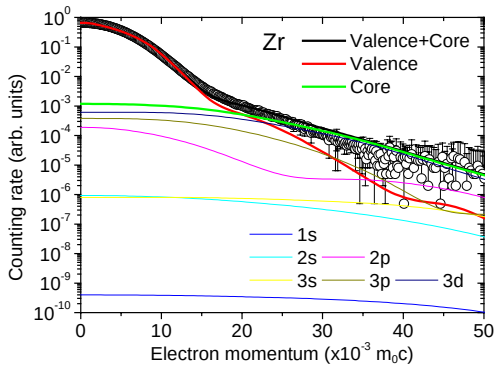

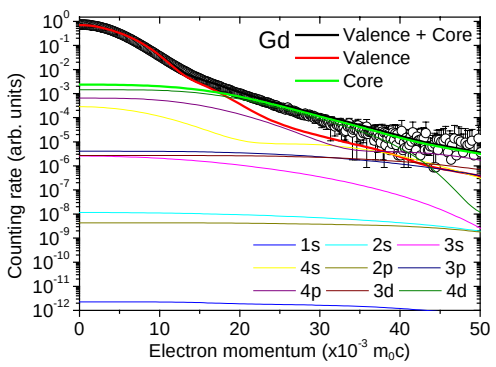

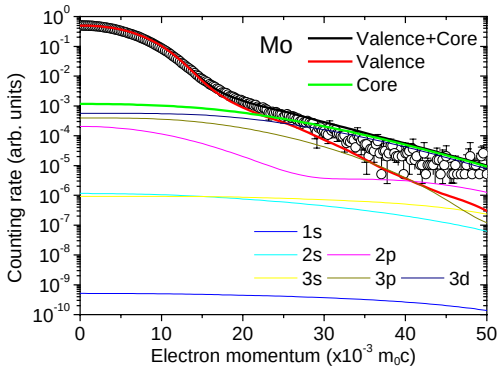

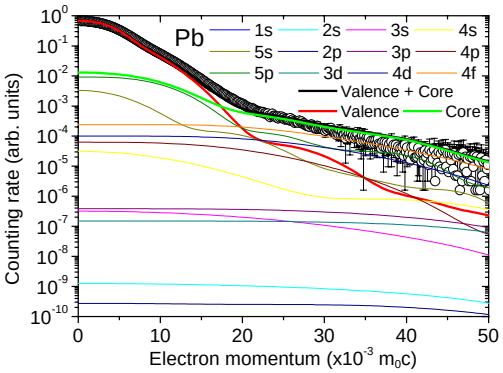

Figure 6. DBAR spectra for the Zr and Mo samples (the fifth period). Open circles and solid lines denote measured and calculated spectra, respectively.

Figure 7. DBAR spectrum for the Gd and Pb samples (the sizth period). Open circles and solid lines denote measured and calculated spectra, respectively.

References

[1] Ishibashi S 2004 *Mater. Sci. Forum* **445-446** 401-403.
[2] Blöhl P E 1994 *Phys. Rev.* B**50** 17953-17979.
[3] Puska M J and Nieminen R M 1994 *Rev. Mod. Phys.* **66** 841–897.
[4] Gonze X, Beuken J -M, Caracas R, Detraux F, Fuchs M, Rignanese G -M, Sindic L, Verstraete M, Zerah G, Jollet F, Torrent M, Roy A, Mikami M, Ghosez Ph, Raty J -Y, and Allan D C 2002 *Comput. Mater. Sci.* **25** 478–492.
[5] Holzwarth N A W, Tackett A R and Matthews G E 2001 *Comput. Phys. Commun.* **135** 329–347.
[6] Clementi E and Roetti C 1974 *At. Data Nucl. Data Tables* **14** 177-478.
[7] Borónski E and Nieminen R M 1986 *Phys. Rev.* B **34** 3820–3831.
[8] Alatalo M, Asoka-Kumar P, Ghosh V J, Nielsen B, Lynn K G, Lruseman A C, Van Veen A, Korhonen T, and Puska M 1998, *J. Phys. Chem.* **59** 55-59.